structure was discretized on a cubic mesh with 28 cells in the diameter of the circular waveguide. The S-parameters are shown in fig. 3b, along with results obtained with a mode matching approach. Similar TLM results can be obtained with one-way equation ABC's, although there is always the potential for instabilities with this type of boundary.

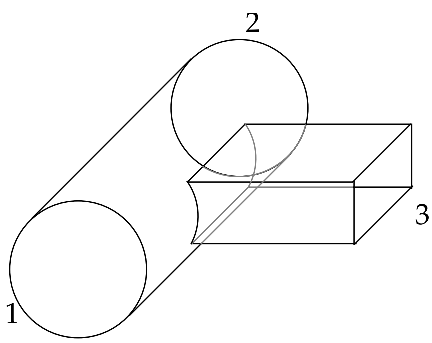

Fig.3a – Geometry of the circular to sidecoupled rectangular waveguide T-junction. Radius: 7.0 mm, rectangular waveguide: WR-62 (16.0 mm by 8.0 mm)

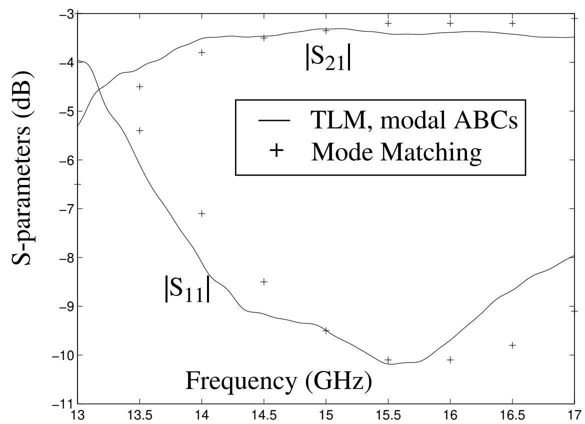

Fig.3b – Magnitude of the S-parameters of the circular to sidecoupled rectangular waveguide T-junction.

Further details can be found in:

J. L. Herring, M. Righi, W.J.R. Hoefer, "Modal Boundary Conditions For Waveguides of Arbitrary Cross-section With SCN TLM" in 1997 Intl. Microwave Symposium Dig., pp. 325-328, Denver, Colorado, June 9-13, 1997.

5) RF drying of softwood lumber in collaboration with the Faculty of Wood Science in UBC

(Mario Righi, Jonathan Herring, Wolfgang J. R. Hoefer and UBC team)

In the course of this research project a time domain model for the RF drying of wood in a vacuum kiln has been developed. The model includes the following physical phenomena involved in the drying of wood:

- Electromagnetic field distribution in the wood and the surrounding kiln,
- Energy deposition which increases the mobility of moisture in the lumber,
- Heat transfer and
- Mass transfer which, in turn, changes the dielectric properties of the wood.

The project aims at coupling all these phenomena in a self-consistent numerical model in space and time. Validation of the simulated results will be performed using the experimental RF/Vacuum Kiln available at UBC.

In order to cast the numerical models into a form directly amenable to experimental verification, the algorithms were implemented for a geometry resembling that of the UBC experimental kiln which is shown in Fig. 1. For modeling convenience, the parallel plates containing the wood sample were placed in a rectangular rather than circular cavity.

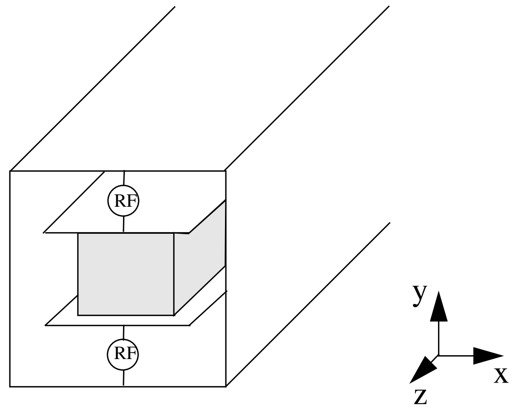

Figure 1. UBC RF kiln

The size of the wood sample is about 1 by 1 by 8 feet. Symmetry along the three axes has been exploited: only one-eighth of the structure needs to be considered, which leads to considerable savings. The electromagnetic as well as the thermal and mass transfer models are stand-alone FORTRAN programs which can exploit public domain plotting routines for interactive visualization (e.g. PLPLOT).

The algorithm modeling the interaction between the electromagnetic solver and the heat/moisture diffusion solver is shown in Fig. 2.

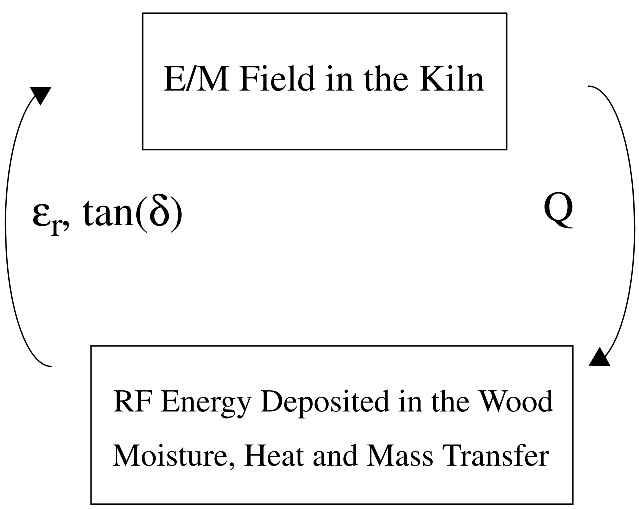

$$\nabla\times\boldsymbol{E} = -\frac{\partial}{\partial t}(\mu_r \boldsymbol{H})$$

$$\nabla\times\boldsymbol{H} = \boldsymbol{j} + \frac{\partial}{\partial t}(\varepsilon_r \boldsymbol{E})$$

$$\frac{\partial M}{\partial t} = \nabla\,(D_M \nabla M) + \nabla\,(D_T \nabla T)$$

$$\rho c \frac{\partial T}{\partial t} = \nabla\,(\lambda_T \nabla T) + \nabla\,(\lambda_M \nabla M) + Q$$

Figure 2 Modeling algorithm for the coupled electromagnetic/heat diffusion/moisture diffusion phenomena, and the differential equations governing them.

The algorithm can be summarized as follows:

a) The thermal mesh and the EM mesh are arranged so that they overlap each other;

b) The electromagnetic field, temperature and moisture are available in each cuboid mesh cell, at each time step;

c) The electromagnetic field in every point in the kiln is computed with TLM;

d) The RF power dissipated in each cuboid is fed as source into the thermal code;

e) One time step at a time in the thermal code is performed (diffusion of heat and moisture) in the wood until a change in material parameters (ε' and tan(δ) is detected;

f) The new parameters are returned to the electro-magnetic TLM code to generate the new field configuration.

These cycle is repeated until the wood is dry.

Characteristics of the Electromagnetic Code

The electromagnetic code is based on the TLM method in the cuboid formulation. Stubs are added to the elementary node in order to model the anisotropic properties of the wood. Because the placement of the wood in the kiln usually aligns the wood fibers with the kiln axis, only diagonal tensors for the permittivity and permeability are necessary. Time varying ε' and tan(δ) are con-sidered and can be specified through interpolated functions (related to the temperature and moisture content in that region of wood) or by look-up tables. In this way different wood species and other biopolymers can be modeled. Boundary conditions are given by the kiln and electrode geometry.

Characteristics of the Thermal Code

The thermal code model is a discrete formulation of the heat and moisture diffusion processes. The equations governing these processes are given in the lower right quadrant of Figure 2. In these equa-tions ρ is the wood density, c is the wood specific heat, T is the temperature in the wood, M is the moisture content and Q is the heat deposited by the radio frequency electromagnetic fields. The coefficients D_M, D_T, λ_M, λ_T are the diffusivity coefficients for the moisture content and the heat.

The presence of these coefficients means that the heat and moisture diffusion can occur because of the gradients of both heat and moisture. Based on the input received by Dr. Avramidis and his group at UBC the equations can be simplified as:

$$\frac{\partial M}{\partial t} = \nabla\ (D_M \nabla\, M)$$

$$\rho c \frac{\partial T}{\partial t} = \nabla\ (\lambda_T \nabla\, T) + Q$$

The above differential equations have been discretized using Finite Differences in the Time Domain (FDTD) based on the FTCS (Forward Time Central Space) scheme. Cuboid nodes and anisotropic properties (diagonal tensor) have been implemented. Inhomogenous regions are also considered. All above parameters can be time varying, and can be specified as functions of moisture, temperature, fiber saturation point, etc. either as look-up tables or as specified functions.

As the diffusion evolves, the dielectric properties of the material change, and the new properties are fed back to the electromagnetic solver to compute the new field distribution. In order to ensure an accurate tracking of the field as it evolves in the wood, only small changes in moisture and temperature distribution are allowed. This is accomplished by using an adaptive time step for the diffusion phenomena. The time step at each iteration of the thermal code is computed so that the change in properties is smaller than 1%.

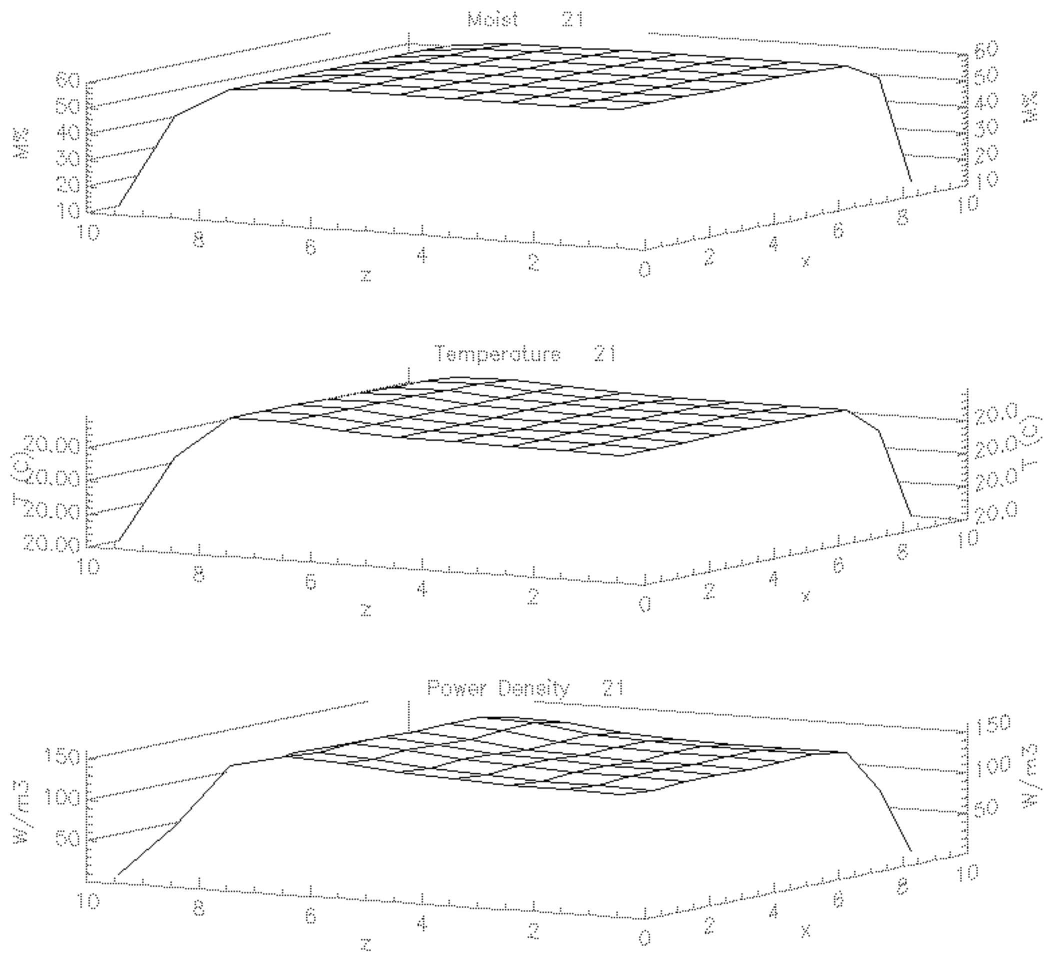

Figure 3. Moisture, temperature and power density in 1/8 of the wood sample at time step 21.

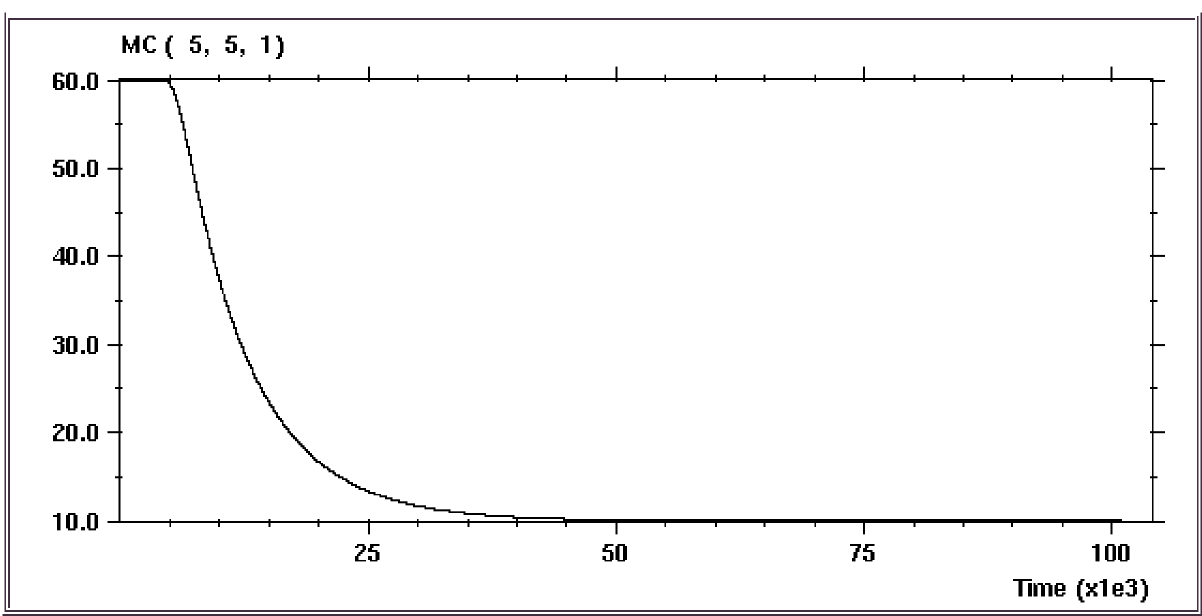

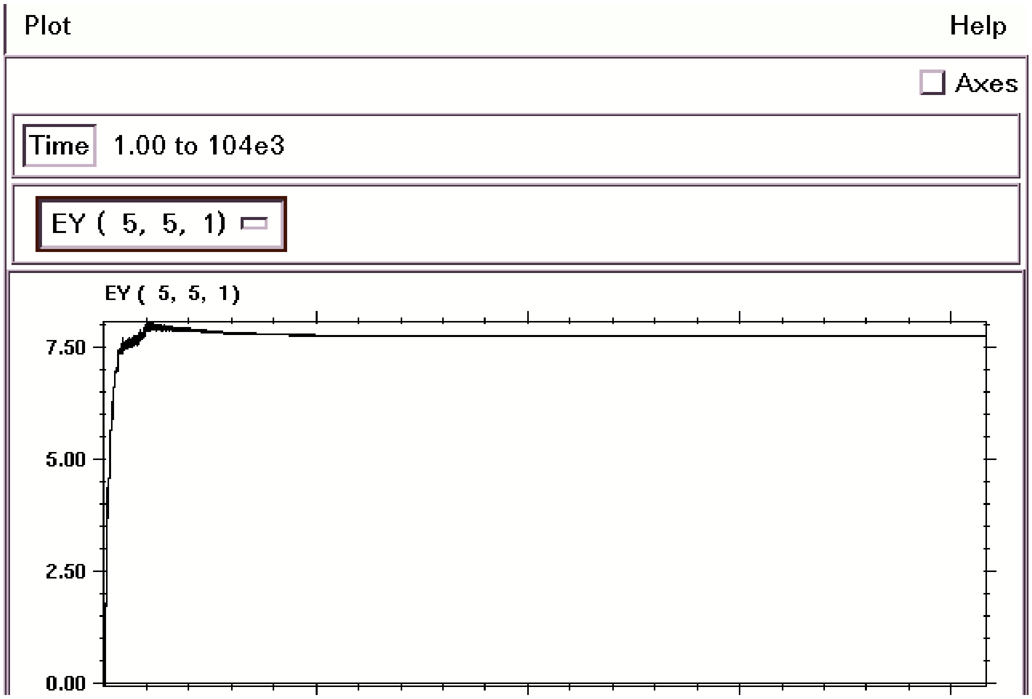

Figure 4. Results obtained during step 1. Constant parameters. Moisture content in % (previous page) and electric field strength at a point in the wood sample.

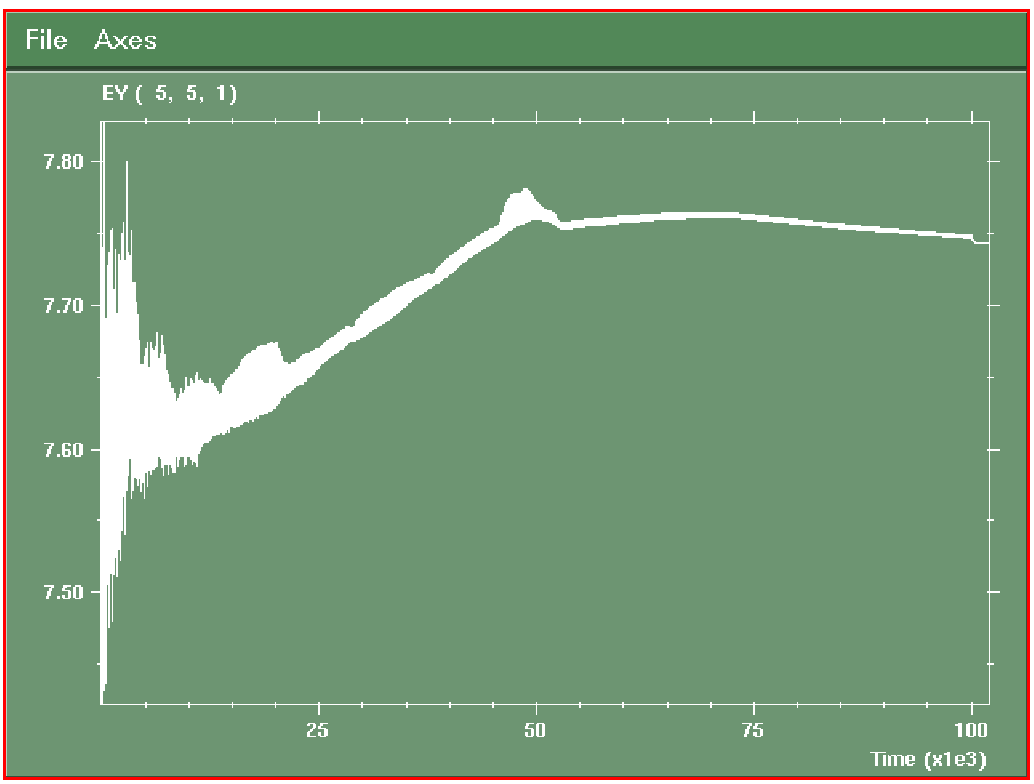

Figure 5. Results obtained during step 2. Variable parameters. Electric field strength at a point inside the wood sample.

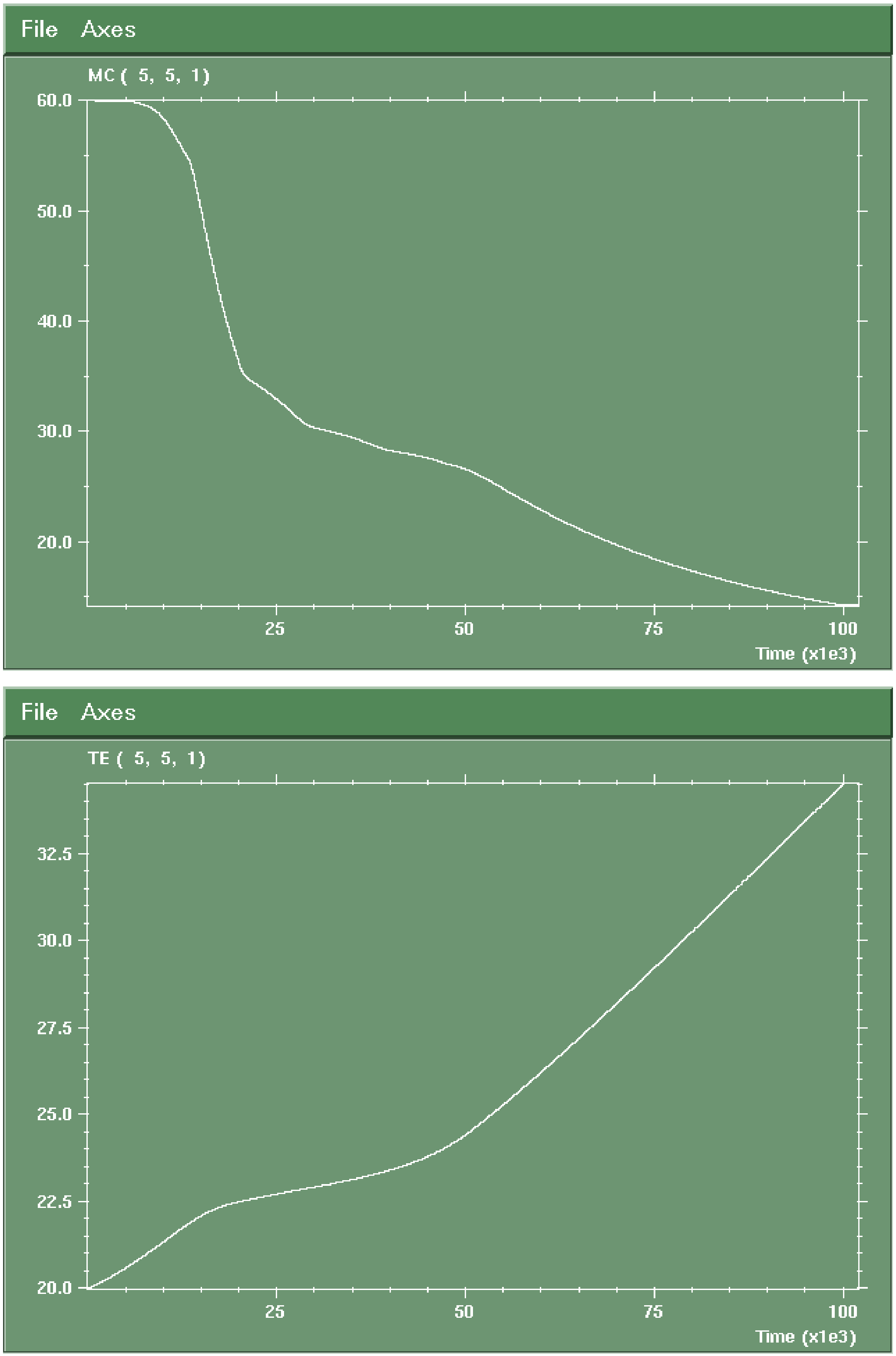

Figure 6. Results obtained during step 2. Variable parameters. Moisture content in % and temperature at a point in the wood sample.

In this way fast and slow diffusion can be always tracked with a suitable time step. The time step can therefore change during the duration of the simulation, while always remaining below the stability limit for the difference scheme given by:

$$\Delta t_{max} \leq \frac{1}{2\left(\frac{D_x}{\Delta x^2} + \frac{D_y}{\Delta y^2} + \frac{D_z}{\Delta z^2}\right)} \qquad \text{Moisture diffusion}$$

$$\Delta t_{max} \leq \frac{1}{2\left(\frac{\lambda_x}{\Delta x^2} + \frac{\lambda_y}{\Delta y^2} + \frac{\lambda_z}{\Delta z^2}\right)} \qquad \text{Heat diffusion}$$

The boundary conditions are imposed according to the initial temperature and moisture in the wood.

Results can be shown interactively, or at the end of the simulation. Figure 3 shows a typical interactive plot showing the moisture, temperature and power density in 1/8 of the wood sample. The initial phases of the diffusion can clearly be identified.

The development of the linkage between the thermal and electromagnetic codes was pursued in two steps. In step one, the thermal and electromagnetic codes were connected while maintaining all parameters in the diffusion equations constant. Results obtained under this simplified condition are shown in Figure 4.

In step two, time-varying, non-constant parameters were used in the diffusion equations to represent the actual process. Results for this conditions are shown in Figures 5 and 6. While these results show a physically consistent behavior, their accuracy depends critically upon the accuracy with which the diffusion parameters can be determined. Research and experimental investigations are in progress at UBC in order to gain more confidence in the accuracy of these results. The plan is to run careful measurements in UBC's experimental RF/Vacuum Kiln. This kiln is presently being fitted with a new power amplifier as energy source, and with new matching networks to maximize power transfer to the sample. During experiments, incident RF power will be kept constant, pressure and temperature are monitored locally, and moisture content will be measured globally in the sample.